Virtual Yaw Rate Display for Reducing Steering Instability of Remote Driving

Junji Ohgashira * **Yuichi Tazaki** * **Hikaru Nagano** *
Yasuyoshi Yokokohji * **Shota Kameoka** **

* *Kobe University, 1-1, Rokko-dai, Nada-ku, Kobe-shi, Hyogo, Japan (e-mail: tazaki@mech.kobe-u.ac.jp).*
** *Mitsubishi Electric, Advanced Technology R&D Center, Tsukaguchi-honmachi, Amagasaki-shi, Hyogo, Japan*

Abstract: In vehicle teleoperation, reducing instability of driving caused by communication delay is one of important technical problems. This study proposes a passivity-based vehicle teleoperation system that compensates for the delay of visual information presented to the driver. The proposed method applies wave variable transformation to steering angle and yaw rate, and presents modified yaw rate to the driver by altering the viewing direction of camera images. This effectively makes the driver feel that the vehicle responds to his/her steering operation without delay, and consequently over-steering is greatly reduced. The results of experiments using a driving simulator showed that the proposed method greatly improves lateral stability of driving.

Keywords: Remote Driving, Teleoperation, Wave Transformation, Delay Compensation

1. INTRODUCTION

To mitigate various problems related to modern transportation systems such as accidents, lack of trained drivers, and congestions, autonomous driving technology has attracted great attention. There are a number of possible traffic scenes in which autonomous driving might not function properly. For example, an autonomous driving system may fail in scenes of emergency such as accidents and disaster where the environment is greatly altered from pre-recorded roadmaps. Moreover, it may also fail to function properly in private zones and unstructured roads where general traffic rules do not apply. For these reasons, remote driving (i.e., vehicle teleoperation) technology is expected to work as a backup of autonomous driving systems in unexpected situations.

One of the major drawbacks of remote driving is deterioration of driving performance compared to onboard driving due to communication delay and lack of sensory information. In particular, communication delay forces the remote driver to steer the vehicle by watching delayed images and causes lateral instability. Predictive display has been studied as a method to mitigate the negative influence of communication delay (Davis et al. (2010); Chucholowski et al. (2013); Chucholowski (2015); Matheson et al. (2013); Brudnak (2016)).

On the other hand, passivity-based delay compensation method has been widely studied in the field of bilateral teleoperation of robotic manipulators (Anderson and Spong (1988); Yokokohji et al. (1999); Niemeyer and Slotine (2004)). By transforming input and output variables (typically velocity and force in the context of bilateral teleoperation) into wave variables before transmitting them over a delayed communication channel, the overall communication channel can be made passive. Assuming that both the operator and the robot are passive, the stability of the overall teleoperation system is guaranteed. Some studies extended the passivity-based framework to teleoperation of vehicles, such as UAV (Lam et al. (2008)) and electric vehicle (Ma et al. (2009); Boukhnifer et al. (2011)). However, these studies do not depart from the basic formulation in which transmitted variables are velocity and force.

Human driver heavily relies on visual information for steering the vehicle, and therefore, a major reason for instability is delay of visual information. To the authors' knowledge, however, a method for compensating the delay of visual information based on wave-variable transformation has not been reported in the literature. In this study, we propose a novel passivity-based vehicle teleoperation method that can compensate for the delay of visual information. A key idea is to apply wave variable transformation to steering angle and yaw rate, instead of velocity and force. Delayed camera images are displayed to the driver from virtual viewing directions in order to make the driver perceive modified yaw rate. The effectiveness of the proposed method is tested through experiments where a number of subjects drove a vehicle in a simulation environment and performed driving tasks consisting of path-tracking and slalom. It has been confirmed that lateral stability of driving could be improved by the proposed method even under a significant delay of 800[ms].

2. REVIEW OF PASSIVITY-BASED TELEOPERATION

In this section, the theoretical basics of passivity-based bilateral teleoperation is briefly reviewed. The wave-variable method was initially proposed as a mechanism to mitigate

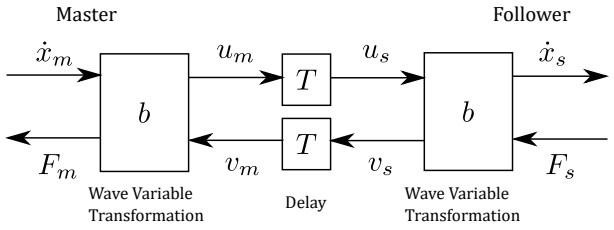

Fig. 1. Classical wave variable transformation

instability of bilateral teleoperation system of robotic manipulators caused by communication delay. In a conventional framework, velocity command is sent from the operator to the remote manipulator, while force is sent back to the operator for realizing force feedback. Oscillation was known to occur if raw velocity and force information was exchanged over a delayed network, since the delay element continuously injects energy into the system. Instead of directly transmitting force and velocity, these variables are transformed into so-called wave variables. With this transformation, the communication channel can be seen as a passive component which only transmits or dissipates energy but never generates it.

Following the notation of Yokokohji et al. (1999), the wave-variable transformation is defined as follows.

$$\begin{aligned} u_m &= \frac{b\dot{x}_m + F_m}{\sqrt{2b}}, \quad v_m = \frac{b\dot{x}_m - F_m}{\sqrt{2b}} \\ u_s &= \frac{b\dot{x}_s + F_s}{\sqrt{2b}}, \quad v_s = \frac{b\dot{x}_s - F_s}{\sqrt{2b}} \end{aligned} \tag{1}$$

Here, $\dot{x}$ and F are velocity and force variables, respectively, while the subscripts $_m$ and $_s$ indicate the master side and the follower side, respectively. Moreover, u and v are wave variables. Here, b is a constant called the characteristic impedance.

The wave variable u_m is sent over a communication channel with the delay of T and received as u_s at the follower side. Similarly, v_s is sent back from the follower side to be received as v_m at the master side. Thus we have:

$$\begin{aligned} u_s(t) &= u_m(t-T), \\ v_m(t) &= v_s(t-T). \end{aligned} \tag{2}$$

The communication channel is said to be passive if the net energy flowed into the channel is either stored or dissipated; that is, if there exists a positive-definite storage function $S(t)$ that satisfies the following:

$$\frac{d}{dt}S(t) \leq \dot{x}_m F_m - \dot{x}_s F_s \tag{3}$$

From (1) and (2), we obtain

$$\dot{x}_m F_m - \dot{x}_s F_s = \frac{d}{dt}\int_{t-T}^{t} \frac{1}{2}\left(u_m^2(\tau) + v_s^2(\tau)\right) d\tau \tag{4}$$

which means that the communication channel is in fact passive with the storage function defined as $S(t) = \int_{t-T}^{t} \frac{1}{2}\left(u_m^2(\tau) + v_s^2(\tau)\right) d\tau$. Since any cascade composition of passive systems are also passive, assuming that the robot and the operator are passive, the entire teleoperation system is guaranteed to be passive and therefore instability will never occur.

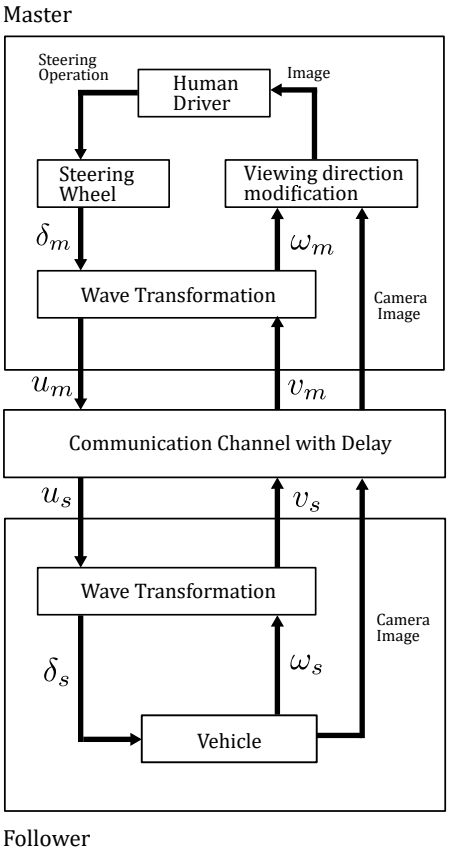

Fig. 2. Remote control system configuration

3. PASSIVITY-BASED VEHICLE TELEOPERATION SYSTEM

3.1 Overall Architecture

A passivity-based vehicle teleoperation system proposed in this paper is described below. A block diagram of the developed system is illustrated in Fig. 2. A fundamental difference from the conventional passivity-based bilateral teleoperation system is that the pair of variables transmitted over the communication channel are steering angle and yaw rate, instead of velocity and force. Therefore, the wave-variable transformation for this system is defined as

$$\begin{aligned} u_m &= \frac{b\delta_m + \omega_m}{\sqrt{2b}}, \quad v_m = \frac{b\delta_m - \omega_m}{\sqrt{2b}}, \\ u_s &= \frac{b\delta_s + \omega_s}{\sqrt{2b}}, \quad v_s = \frac{b\delta_s - \omega_s}{\sqrt{2b}}, \end{aligned} \tag{5}$$

where δ is the steering angle and ω is the yaw rate. Apart from the wave variables, a stream of images captured by a camera mounted on the remote vehicle is sent over the communication channel. For simplicity, communication delay of wave variables and that of images are assumed to be constant and have the same value denoted by T. In real teleoperation systems, delay may be time-varying and include gitters. In such cases, buffers could be inserted to communication channels to smooth out the fluctuation of delay. For this reason, we consider that the contant delay assumption is acceptable from a practical point of view.

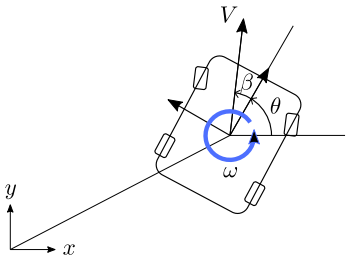

Fig. 3. Definition of heading, yaw rate, and slip angle.

Table 1. List of symbols

Symbol	Definition	Unit
β	Slip angle	rad
θ	Heading angle	rad
ω	Yaw rate	rad/s
V	Speed	m/s
m	Total mass	kg
I	Moment of inertia around CoG	$kg \cdot m^2$
l_f	Distance between CoG and front axle	m
l_r	Distance between CoG and rear axle	m
K_f	Cornering stiffness of front tyres	N/rad
K_r	Cornering stiffness of rear tyres	N/rad
δ	Steering angle of front wheel	rad

3.2 Vehicle Dynamical Model

The dynamical model of the vehicle is described as follows. Related symbols are listed in Table 1. The vehicle is modeled as a single rigid body moving on a ground plane, where its vertical movement and roll and pitch rotations are neglected. As illustrated in Fig. 3, the heading angle of the vehicle relative to the x-axis of the global coordinate frame is defined as θ, and its derivative ω is called the yaw rate. The angle between the vehicle's heading direction and the direction of its velocity vector is defined as the slip angle β. We assume that the longitudinal speed V is constant, and that β is sufficiently small (i.e., $|\beta| \ll 1$). Under these assumptions, the lateral acceleration of the vehicle expressed in the vehicle's local coordinate frame is given by $V(\omega + \dot{\beta})$.

The slip angle of each tyre is defined as the angle between the tyre's longitudinal direction and the direction of the point velocity of the vehicle at the position of that tyre. Thus we have

$$\begin{aligned} \beta_f &= \tan^{-1}\left(\frac{V\sin\beta + l_f\omega}{V\cos\beta}\right) - \delta \approx \beta + \frac{l_f\omega}{V} - \delta, \\ \beta_r &= \tan^{-1}\left(\frac{V\sin\beta - l_r\omega}{V\cos\beta}\right) \approx \beta - \frac{l_r\omega}{V}. \end{aligned} \tag{6}$$

Lateral force applied to each tyre from the ground is given by the slip angle of that tyre multiplied by the cornering stiffness.

$$\begin{aligned} Y_{f1} = Y_{f2} &= -K_f\beta_f, \\ Y_{r1} = Y_{r2} &= -K_r\beta_r. \end{aligned} \tag{7}$$

The lateral and rotational equation of motion of the vehicle is expressed as follows.

$$\begin{aligned} mV(\dot{\beta} + \omega) &= Y_{f1} + Y_{f2} + Y_{r1} + Y_{r2}, \\ I\dot{\omega} &= l_f(Y_{f1} + Y_{f2}) - l_r(Y_{r1} + Y_{r2}). \end{aligned} \tag{8}$$

Let us define the state variable as $x = \begin{bmatrix}\beta \\ \omega\end{bmatrix}$ and the control input as $u = \delta$. Then, by substituting (6) and (7) into (8),

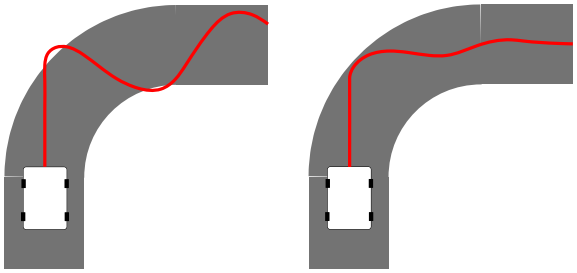

(a) Without proposed method (b) With proposed method

Fig. 4. Illustration of typical cornering behavior

we obtain a linear state equation

$$\dot{x} = Ax + Bu \tag{9}$$

where

$$\begin{aligned} A &= \begin{bmatrix} A_{11} & A_{12} \\ A_{21} & A_{22} \end{bmatrix} \\ &= \begin{bmatrix} -\dfrac{2(K_f + K_r)}{mV} & -1 - \dfrac{2(l_fK_f - l_rK_r)}{mV^2} \\ -\dfrac{2(l_fK_f - l_rK_r)}{I} & -\dfrac{2(l_f^2K_f + l_r^2K_r)}{IV} \end{bmatrix}, \\ B &= \begin{bmatrix} B_1 \\ B_2 \end{bmatrix} = \begin{bmatrix} \dfrac{2K_f}{mV} \\ \dfrac{2l_fK_f}{I} \end{bmatrix}. \end{aligned}$$

Observe that in a special case where $l_fK_f = l_rK_r$ holds, the A matrix becomes diagonal, and as a result, the dynamics of β and ω become two parallel subsystems driven by the common input u:

$$\dot{\beta} = A_{11}\beta + B_1u \tag{10}$$

$$\dot{\omega} = A_{22}\omega + B_2u \tag{11}$$

and since A_{11} and A_{22} are both negative, the open-loop dynamics of these subsystems are both asymptotically stable. Note that $l_fK_f = l_rK_r$ is called the neutral steer condition, whereas $l_fK_f > l_rK_r$ and $l_fK_f < l_rK_r$ are called over-steer and under-steer, respectively.

Let us define a Lyapunov function of the ω-subsystem as

$$V(\omega) = \frac{1}{2B_2}\omega^2 \tag{12}$$

Then we have

$$\frac{d}{dt}V(\omega) = \frac{1}{B_2}\omega\dot{\omega} = \frac{A_{22}}{B_2}\omega^2 + \omega\delta \le \omega\delta \tag{13}$$

which implies that the ω subsystem is in fact passive with the storage function $V(\omega)$. Based on this observation, in this study, we assume that the remote vehicle satisfies the neutral-steer condition and focus on the stability of ω.

3.3 Image Presentation Method

As described earlier, our idea is to construct a remote driving system in which the steering angle δ and the yaw rate ω are transmitted variables. A key challenge here is how to display the transformed yaw rate ω_m to the human driver. Our idea is to modify the viewing direction of camera images so that the driver perceives ω_m from displayed stream of images.

From (5), the yaw rate ω_m which must be displayed to the driver, is given as follows.

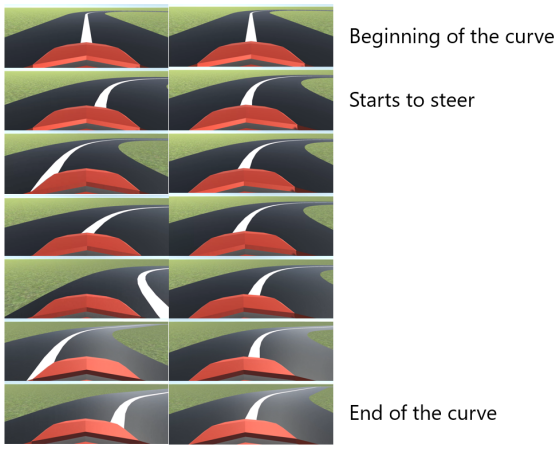

Fig. 5. Comparison of driver's view during driving through a curve. Without the proposed method, the vehicle heading sways unsteadily (left). With the proposed method, the vehicle heading turns swiftly in response to the driver's steering at the beginning of the curve, and remains steady throughout (right).

$$\omega_m(t) = \omega_s(t-T) + b(\delta_m(t) - \delta_s(t-T)) \qquad (14)$$

By integrating ω_m, we obtain the absolute yaw angle θ_m as follows.

$$\theta_m(t) = \int_0^t \omega_m(\tau)d\tau \qquad (15)$$

There are two possible ways to modify the viewing direction of camera images presented to the driver, depending on whether this mechanism is implemented in a simulation environment or in a real vehicle system. In the former case, implementation is relatively simple, since the absolute viewing direction θ_m can be directly specified, and virtual view in that viewing direction can be rendered as computer graphics and displayed to the driver. In the latter case, if the camera image is displayed without any modification, the driver will perceive (by his/her own visual processing) $\omega_s(t-T)$, which is the vehicle's yaw rate at the instant the image was captured. In order to let him/her perceive $\omega_m(t)$ instead of $\omega_s(t-T)$, we need to modify the perceived yaw rate by $\omega_e(t) := \omega_m(t) - \omega_s(t-T) = b(\delta_m(t) - \delta_s(t-T))$. If the camera mounted on the vehicle is an omni-directional camera and images are displayed on a cylindrical screen, then additional yaw rate could be displayed by simply turning the image along the axis of the cylinder with the angular velocity $-\omega_e$. In this study, we have actually implemented and tested this image presentation method in a simulation environment. Implementing on a real vehicle system is considered to be a subject of future study.

Figures 4(a),(b) illustrate typical cornering behavior with and without the proposed method. Moreover, Figs. 5 shows snapshot images of the driver's view during cornering. Without the proposed method, the vehicle's response to the driver's steering perceived in the image is delayed, and therefore the driver tends to increase steering more than necessary. This results in a winding path illustrated in Fig. 4(a). With the prposed method, on the other hand, we can see in (14) that $\omega_m(t)$ is influenced by $\delta_m(t)$ with no delay. Therefore, by displaying camera images in a virtual viewing direction θ_m, the driver's steering operation will be directly reflected to the viewing direction without delay.

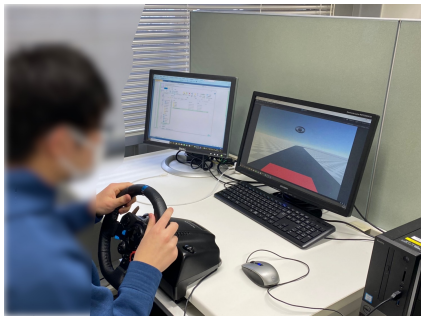

Fig. 6. View of the experimental setup.

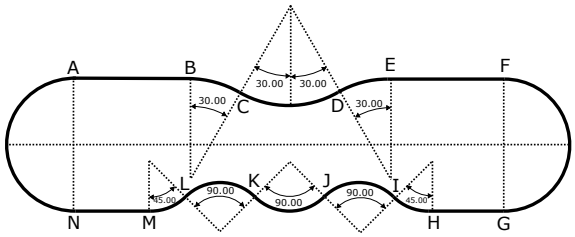

(a) Course for path-tracking task

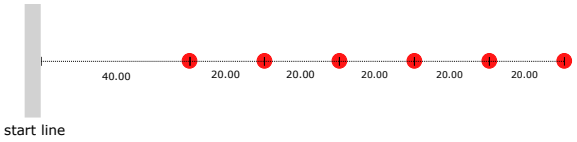

(b) Course for slalom task

Fig. 7. Test course constructed in simulation environment

This will make the driver feel that the vehicle actually responded to his/her steering swiftly. As a result, over-steering which could lead to instability of driving will be reduced, as illustrated in Fig. 4(b).

3.4 Setting of Characteristic Impedance

The characteristic impedance b should be chosen carefully depending on the dynamics of the vehicle. In the case of our vehicle teleoperation system, b is multiplied to the steering angle to determine the amount of adjustment of yaw rate. Based on this observation, we set b as the ratio between a constant steering angle and the corresponding steady-state yaw rate, that is, $b = -\frac{B_2}{A_{22}}$.

4. EXPERIMENTS

Experiments were conducted to verify the effectiveness of the proposed passivity-based vehicle teleoperation system. In this experiment, the dynamical behavior of the vehicle was computed using the linear dynamical system model described in Section 3.2. The view from the vehicle was rendered as computer graphics and displayed to the driver (Fig. 6). The driver controlled the lateral behavior of the vehicle by operating a steering wheel, while the longitudinal speed of the vehicle was automatically kept constant during driving. Synthetic communication delay was generated inside a computer program, and actual network communication was not performed.

Each subject performed two driving tasks, one the path-tracking task, which is to drive along a cyclic course shown

Table 2. Experiment setting

setting	0	1	2	3	4
delay[ms]	0	400	400	800	800
proposed method		none	apply	none	apply

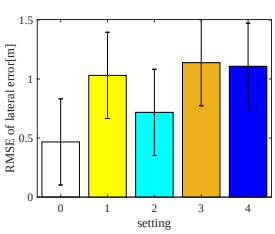

(a) Lateral error

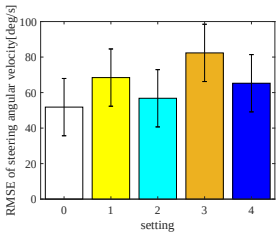

(b) Steering angular velocity

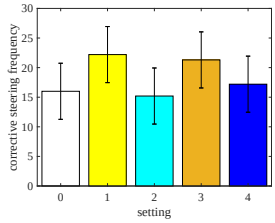

(c) Corrective steering frequency

Fig. 8. Results of the path-tracking task

in Fig. 7(a), and the other is the slalom task, which is to drive between equally spaced poles shown in Fig. 7(b). The driving speed was fixed to 17[km/h]. Two settings of round-trip delay were considered: 400[ms] and 800[ms].

For each task, two trials were performed for each setting shown in Table 2. In order to become familiarized with driving without delay, each subject went through practice sessions consisting of three laps of each task. In the path-tracking task, the subject was asked to keep the vehicle on the center line of the lane as much as possible. In the slalom task, to avoid collision with poles and driving outside the poles was assigned higher priority, while driving through the middle of poles with small turns as much as possible was assigned lower priority.

The results of the path-tracking task is shown in Figs. 8(a)-(c). The figures show lateral error, absolute steering angular velocity, and the number of corrective steering, respectively. Each bar indicates the average, while the error bar vertical line indicates the standard deviation. In terms of all evaluation measures, the result with the proposed delay compensation method showed better score compared to the result without it. The proposed method makes the viewing direction change immediately in response to the driver's steering operation. This characteristic is considered to have enabled the driver to steer the vehicle intuitively. In fact, in the questionnaires, several subjects commented that they could drive without strongly feeling the presence of delay with the help of the proposed method.

The recorded trajectory of the vehicle operated by one of the subjects under the 400[ms] delay is shown in Figs. 9(a),(b). The driver was unable to steer the vehicle properly at steep curves, and the vehicle greatly deviated from the path. In contrast, with the support of the proposed method, the driver was able to track the path with out much deviation just like onboard driving. The recorded

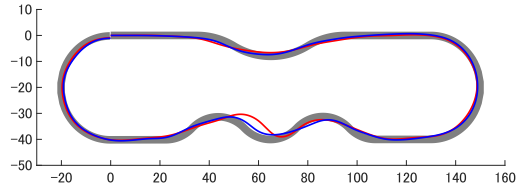

(a) Without proposed method

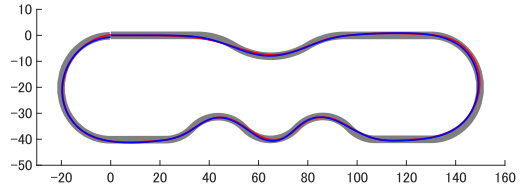

(b) With proposed method

Fig. 9. Course driving route at 400ms for a subject

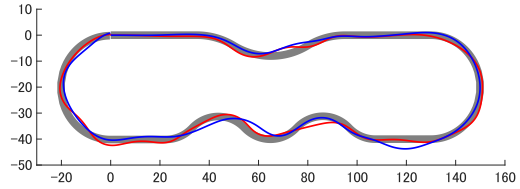

(a) Without proposed method

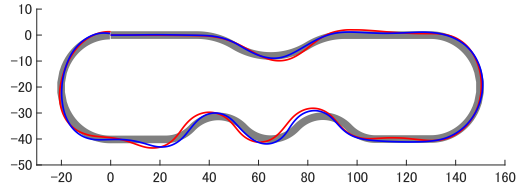

(b) With proposed method

Fig. 10. Course driving route at 800ms for a subject

vehicle trajectory operated by the same subject under the 800[ms] delay is shown in Figs. 10(a),(b). Without delay compensation, the vehicle deviated from the path not only at steep curves but also at milder curves and straight tracks. With the proposed method, the overall tracking error is greatly reduced, but lateral error at steep curves is still significant. This indicates that although the proposed method reduces oscillatory behavior of steering, it does not necessarily improve the accuracy of path tracking under large delay.

The result of the slalom task is shown in Figs. 11(a)-(c). Similar to the path-tracking task, in the 400[ms] delay setting, the result with the proposed method showed better performance in all evaluation measures. It can also be observed in Fig. 12(b) that smooth slalom was performed with the help of the proposed method, although the trajectory is slightly shifted to the right because of delay. In the 800[ms] delay setting, however, lateral error was greater when the proposed method was used, and lateral deviation is also clearly seen in actual trajectories shown in Figs 13(a),(b). As discussed in earlier, the proposed method effectively suppresses steering instability but does not necessarily improves tracking accuracy. For this reason, in the slalom task with 800[ms] delay, the vehicle's turning was delayed and its trajectory was shifted to the right in the figure. As a result, the vehicle's trajectory was

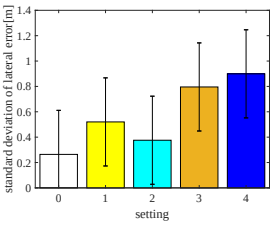

(a) Lateral error

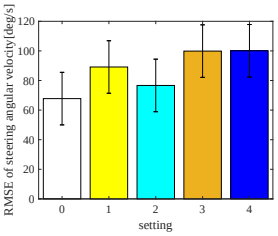

(b) Steering angular velocity

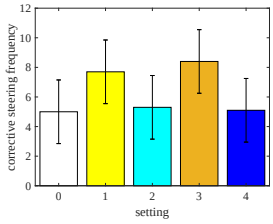

(c) Corrective steering frequency

Fig. 11. Results of the slalom task

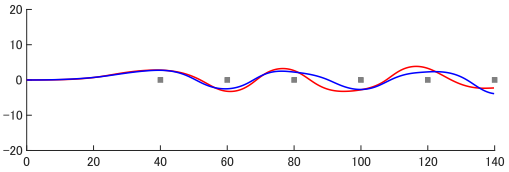

(a) Without proposed method

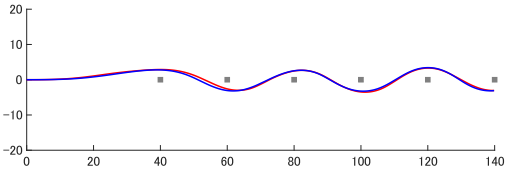

(b) With proposed method

Fig. 12. Pylon slalom driving route at 400ms delay for a subject

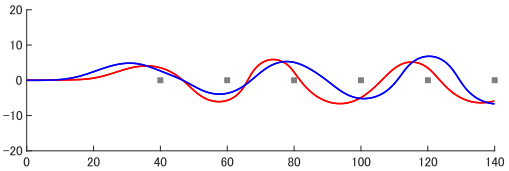

(a) Without proposed method

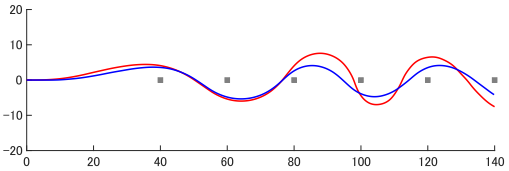

(b) With proposed method

Fig. 13. Pylon slalom driving route at 800ms delay for a subject

forced to swell largely to the sides in order to make the vehicle drive between the poles.

5. CONCLUSION

In this study, we have developed a new passivity-based vehicle teleoperation method which can mitigate instability caused by communication delay. The basic idea of our method is to apply wave variable transformation to steering angle and yaw rate, and present virtual yaw rate to the driver by modifying the viewing angle of camera images. In experiments with small delay, driving with the proposed method showed notable improvement in all measures. It was found, however, that although the proposed method reduces instability of steering, it does not directly improve path-tracking accuracy. This resulted in poor path-tracking performance under large delay. One possible solution for improvement would be to combine the proposed method with predictive display. Other possible directions are extending the proposed method to longitudinal control of the vehicle, and implementing and testing the proposed method in a real remote driving system.

REFERENCES

Anderson, R. and Spong, M. (1988). Bilateral control of teleoperators with time delay. In *Proceedings of the 1988 IEEE International Conference on Systems, Man, and Cybernetics*, volume 1, 131–138.

Boukhnifer, M., Chaibet, A., and Larouci, C. (2011). Passivity based control of teleoperated electric vehicle. *Journal of Asian Electric Vehicles*, 9(1), 1483–1490.

Brudnak, M. (2016). Predictive displays for high latency teleoperation. In *NDIA Ground Vehicle Systems Engineering and Technology Symposium*, 1–16.

Chucholowski, F. (2015). Evaluation of display methods for teleoperation of road vehicles. *The Journal of Unmanned System Technology*, 3(3).

Chucholowski, F., Büchner, S., Reicheneder, J., and Lienkamp, M. (2013). Prediction methods for teleoperated road vehicles. In *Conference on Future Automotive Technology - Focus Electromobility*.

Davis, J., Smyth, C., and McDowell, K. (2010). The effects of time lag on driving performance and a possible mitigation. *IEEE Transactions on Robotics*, 26(3), 590–593.

Lam, T.M., Mulder, M., and Van Paassen, M.M. (2008). Haptic feedback in uninhabited aerial vehicle teleoperation with time delay. *Journal of Guidance, Control, and Dynamics*, 31(6), 1728–1739.

Ma, L., Xu, Z., and Schilling, K. (2009). Robust bilateral teleoperation of a car-like rover with communication delay. In *2009 European Control Conference (ECC)*, 2337–2342.

Matheson, A., Donmez, B., Rehmatullah, F., Jasiobedzki, P., Ng, H.K., Panwar, V., and Li, M. (2013). The effects of predictive displays on performance in driving tasks with multi-second latency: Aiding tele-operation of lunar rovers. In *Proceedings of the Human Factors and Ergonomics Society Annual Meeting*, volume 57, 21–25.

Niemeyer, G. and Slotine, J.J.E. (2004). Telemanipulation with time delays. *The International Journal of Robotics Research*, 23(9), 873–890.

Yokokohji, Y., Imaida, T., and Yoshikawa, T. (1999). Bilateral teleoperation under time-varying communication delay. In *Proceedings 1999 IEEE/RSJ International Conference on Intelligent Robots and Systems*, 1854–1859.